

# Orthonormal Divergence-Free Wavelet Analysis of Energy Transfer in Hall MHD Turbulence

Keisuke ARAKI and Hideaki MIURA<sup>1)</sup>

*Okayama University of Science, 1-1 Ridai-cho, Okayama 700-0005, Japan*

<sup>1)</sup>*National Institute for Fusion Science, 322-6 Oroshi-cho, Toki 509-5292, Japan*

(Received 9 December 2009 / Accepted 4 March 2010)

We studied the basic features of energy transfer in fully developed, freely decaying, isotropic, and homogeneous turbulence in magnetohydrodynamic (MHD) and Hall MHD (HMHD) media using orthonormal divergence-free wavelet analysis. The analysis supports the idea that energy transfer occurs *locally*; i.e., intense energy transfer occurs between modes that have very close spatial scales. The wavelet counterpart of triad interaction analysis in Fourier analysis shows that *local interaction*, i.e., combinations of three wavelet modes that have very close spatial scales, dominates the energy exchange between the velocity and magnetic fields. Energy transfer due to the Hall effect has opposite tendencies at larger and smaller scales, which is consistent with the results of Mininni *et al.* [P.D. Mininni *et al.*, J. Plasma Phys. **73**, 377 (2007)]. At larger scales, it causes a moderate inverse cascade. In contrast, it causes an intense forward cascade at smaller scales.

© 2010 The Japan Society of Plasma Science and Nuclear Fusion Research

Keywords: Hall magnetohydrodynamics, fully developed turbulence, wavelet analysis, energy transfer

DOI: 10.1585/pfr.5.S2048

## 1. Introduction

Though the single-fluid magnetohydrodynamic (MHD) equations are considered a good platform for studying macroscopic behaviors of fusion plasmas, some phenomena may be outside the scope of these equations. The roles of two-fluid effects have attracted attention in research areas such as fusion plasmas [1, 2] and astrophysical plasmas [3, 4]. Hall MHD (HMHD) is known as a simple fluid model that includes a two-fluid effect. The features of turbulent energy transport in HMHD systems were investigated by Mininni *et al.* using Fourier analysis [5].

The purpose of the present work is to determine the basic features of energy transfer due to nonlinear interactions, magnetic induction, and Hall term effects using wavelet analysis. Only the spatial scale information on wavelets is used here, although they also have information on location, helicity and anisotropy in wavenumber space. Wavelet analysis of mode interactions between different spatial scales has a counterpart in Fourier analysis [6]. Using information on the locations of wavelets, we developed a useful tool to visually illustrate the relationship between coherent structures and the intensity of mode interactions [7, 8]. The location information is extracted by decomposing the integrals given by Eqs. (8), (9), (12), and (13) in section 3. The analysis has no counterpart in Fourier analysis and requires much greater computer resources. Thus, this work is also regarded as a preliminary to more detailed wavelet analysis.

## 2. Basic Equations and Analyzed Data

The incompressible HMHD equations are

$$\frac{\partial \mathbf{u}}{\partial t} + (\mathbf{u} \cdot \nabla) \mathbf{u} = -\nabla P + \mathbf{j} \times \mathbf{b} + \nu \nabla^2 \mathbf{u}, \quad (1)$$

$$\frac{\partial \mathbf{b}}{\partial t} = \nabla \times ((\mathbf{u} - \epsilon \mathbf{j}) \times \mathbf{b}) + \eta \nabla^2 \mathbf{b}, \quad (2)$$

where  $\mathbf{u}$  is the bulk velocity field and satisfies  $\nabla \cdot \mathbf{u} = 0$ ,  $\mathbf{b}$  is the magnetic field,  $\mathbf{j} := \nabla \times \mathbf{b}$  is the current density field,  $P$  is the total pressure,  $\nu$  is the kinematic viscosity,  $\eta$  is the resistivity, and  $\epsilon$  is the parameter for the relative strength of the Hall term. In the present study, the parameters are set to  $\nu = \eta = 2 \times 10^{-3}$  and  $\epsilon = 0.05$ . The case of  $\epsilon = 0$  is studied for comparison.

Here, we analyze the same snapshot data that were used in Miura and Hori [9]. The simulation conditions, the time evolution of the kinetic and magnetic energies, and other details are described in Ref. [9]. Figure 1 shows wavelet-scale spectra of the kinetic and magnetic energies.

## 3. Wavelet-Scale Spectra and Energy Budget Equations

In the present study, we focus on the energy budget of MHD and HMHD for each spatial scale of the velocity and magnetic fields. For this purpose, we carried out scale-to-scale energy budget analysis on the basis of the orthonormal divergence-free wavelets proposed in Ref. [6].

The velocity and magnetic fields are expanded in the wavelet modes as

author's e-mail: araki@are.ous.ac.jp

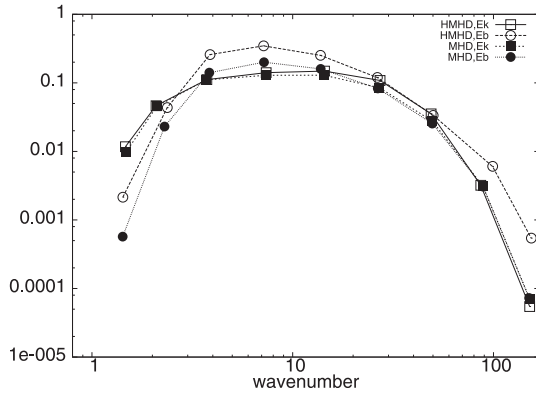


Fig. 1 Wavelet-scale spectra of the kinetic and magnetic energies. Squares:  $E_j^{(u)}$ , circles:  $E_j^{(b)}$ ; open symbols: HMHD, solid symbols: MHD. Abscissas of each quantity are determined according to the mean wavenumber of  $\mathbf{u}_j$  and  $\mathbf{b}_j$ , which is given by  $k_j := \sqrt{\int |\nabla \times \mathbf{f}_j|^2 d^3 \vec{x}} / \int |\mathbf{f}_j|^2 d^3 \vec{x}}$ , where  $\mathbf{f}$  stands for  $\mathbf{u}$ ,  $\mathbf{b}$ .

$$\mathbf{f}(\vec{x}, t) = \sum f_{j\epsilon\vec{l}\sigma}(t) \psi_{j\epsilon\vec{l}\sigma}(\vec{x}), \quad (3)$$

where  $\mathbf{f}$  stands for  $\mathbf{u}$  or  $\mathbf{b}$ ,  $\psi$ 's are the wavelet basis functions, and the expansion coefficients are given by  $f_{j\epsilon\vec{l}\sigma}(t) := \int \mathbf{f}(\vec{x}, t) \cdot \psi_{j\epsilon\vec{l}\sigma}(\vec{x}) d^3 \vec{x}$ . The physical implications of the wavelet indices  $j$ ,  $\epsilon$ ,  $\vec{l}$ , and  $\sigma$  are summarized in Ref. [7]. In the present study, we use only the information on the spatial scale of the wavelets. Thus, the fields are decomposed into a *wavelet-scale spectrum*, which is given by

$$\mathbf{f} = \sum_j \mathbf{f}_j \quad \text{where} \quad \mathbf{f}_j(\vec{x}, t) = \sum_{\epsilon, \vec{l}, \sigma} f_{j\epsilon\vec{l}\sigma}(t) \psi_{j\epsilon\vec{l}\sigma}(\vec{x}). \quad (4)$$

Note that as the scale index  $j$  increases, the corresponding spatial scale becomes smaller by a factor of  $1/2$ .

Substituting the wavelet-scale expansion of  $\mathbf{u}$  and  $\mathbf{b}$  into the basic equations [Eqs. (1) and (2)] and taking the inner product with each of the wavelet-scale spectra  $\mathbf{u}_j$  and  $\mathbf{b}_k$ , respectively, yields the energy budget equations for the scale spectra of the kinetic and magnetic energies, as follows:

$$\begin{aligned} \frac{d}{dt} E_j^{(u)} &= \sum_{k,m} \langle \mathbf{u}_j | \mathbf{u}_m | \mathbf{u}_k \rangle_{\text{NL}} \\ &+ \sum_{k,m} \langle \mathbf{u}_j | \mathbf{b}_m | \mathbf{b}_k \rangle_{\text{Lor}} + \sum_k D_{jk}, \end{aligned} \quad (5)$$

$$\begin{aligned} \frac{d}{dt} E_k^{(b)} &= \sum_{j,m} \langle \mathbf{b}_k | \mathbf{b}_m | \mathbf{u}_j \rangle_{\text{Ind}} \\ &+ \sum_{j,m} \langle \mathbf{b}_k | \mathbf{b}_m | \mathbf{b}_j \rangle_{\text{Hall}} + \sum_k R_{kj}, \end{aligned} \quad (6)$$

where the subindices of the brackets NL, Lor, Ind, and Hall stand for nonlinear interaction, the Lorentz force, magnetic induction, and the Hall effect, respectively. The  $E_j$  values and brackets, respectively, are defined by the integrals

$$E_j^{(u)} := \frac{1}{2} \int \mathbf{u}_j \cdot \mathbf{u}_j d^3 \vec{x}, \quad (7)$$

$$\langle \mathbf{u}_j | \mathbf{u}_m | \mathbf{u}_k \rangle_{\text{NL}} := - \int \mathbf{u}_j \cdot ((\mathbf{u}_m \cdot \nabla) \mathbf{u}_k) d^3 \vec{x}, \quad (8)$$

$$\langle \mathbf{u}_j | \mathbf{b}_m | \mathbf{b}_k \rangle_{\text{Lor}} := \int \mathbf{u}_j \cdot (\mathbf{j}_k \times \mathbf{b}_m) d^3 \vec{x}, \quad (9)$$

$$D_{jk} := \nu \int \mathbf{u}_j \cdot \nabla^2 \mathbf{u}_k d^3 \vec{x}, \quad (10)$$

$$E_k^{(b)} := \frac{1}{2} \int \mathbf{b}_k \cdot \mathbf{b}_k d^3 \vec{x}, \quad (11)$$

$$\langle \mathbf{b}_k | \mathbf{b}_m | \mathbf{u}_j \rangle_{\text{Ind}} := \int \mathbf{b}_k \cdot \nabla \times (\mathbf{u}_j \times \mathbf{b}_m) d^3 \vec{x}, \quad (12)$$

$$\langle \mathbf{b}_k | \mathbf{b}_m | \mathbf{b}_j \rangle_{\text{Hall}} := -\epsilon \int \mathbf{b}_k \cdot \nabla \times (\mathbf{j}_j \times \mathbf{b}_m) d^3 \vec{x}, \quad (13)$$

$$R_{kj} := \eta \int \mathbf{b}_k \cdot \nabla^2 \mathbf{b}_j d^3 \vec{x}. \quad (14)$$

and  $\mathbf{j}_k := \nabla \times \mathbf{b}_k$ . The pressure term vanishes because each scale spectrum is divergence-free. In the following equations, the fields that appear in a bracket  $\langle \mathbf{f} |$ ,  $|\mathbf{f}|$ , and  $|\mathbf{f} \rangle$  are called the to-mode, by-mode, and from-mode, respectively.

Integrating by parts shows that these brackets satisfy the following antisymmetric relations:

$$\langle \mathbf{u}_j | \mathbf{u}_m | \mathbf{u}_k \rangle_{\text{NL}} = -\langle \mathbf{u}_k | \mathbf{u}_m | \mathbf{u}_j \rangle_{\text{NL}}, \quad (15)$$

$$\langle \mathbf{u}_j | \mathbf{b}_m | \mathbf{b}_k \rangle_{\text{Lor}} = -\langle \mathbf{b}_k | \mathbf{b}_m | \mathbf{u}_j \rangle_{\text{Ind}}, \quad (16)$$

$$\langle \mathbf{b}_k | \mathbf{b}_m | \mathbf{b}_j \rangle_{\text{Hall}} = -\langle \mathbf{b}_j | \mathbf{b}_m | \mathbf{b}_k \rangle_{\text{Hall}}. \quad (17)$$

The implications of these relations are that the role of the nonlinear term [Eq. (15)] and the Hall term [Eq. (17)] are the redistribution of the kinetic and magnetic energies, respectively. The role of the magnetic induction and Lorentz force terms [Eq. (16)] is mutual conversion of the magnetic and kinetic energies.

In Ref. [8], we discussed in detail the physical foundation of the evaluation of energy transfer between the kinetic and magnetic energies by the integrals of  $\nabla \times (\mathbf{u} \times \mathbf{b})$  and  $\mathbf{j} \times \mathbf{b}$  instead of  $(\mathbf{b} \cdot \nabla) \mathbf{u}$  and  $(\mathbf{b} \cdot \nabla) \mathbf{b}$ . The key to the choice of integrand is the invariance under an arbitrary change in local coordinate system.

## 4. Contribution of Each Term to the Evolution of $E_j^{(u)}$ and $E_j^{(b)}$

Before going into the details of wavelet scale-to-scale energy budget analysis, we present the contribution of each cubic terms in Eqs. (5) and (6) to the evolution of  $E_j^{(u)}$  and  $E_j^{(b)}$ . Figure 2 shows the wavelet counterparts of the transfer function in Fourier analysis. Brackets are summed with respect to the from- and by-modes, e.g.,  $\langle \mathbf{u}_j | \mathbf{b} | \mathbf{b} \rangle_{\text{Lor}} := \sum_{k,m} \langle \mathbf{u}_j | \mathbf{b}_m | \mathbf{b}_k \rangle_{\text{Lor}}$ . The following features appear:

1. For both MHD and HMHD, the nonlinear and Lorentz force terms are positive for  $j = 6, 7, 8$ .
2. Weak nonlinear energy backscatter to larger scales ( $j = 0, 1, 2$ ) is also seen in both cases.

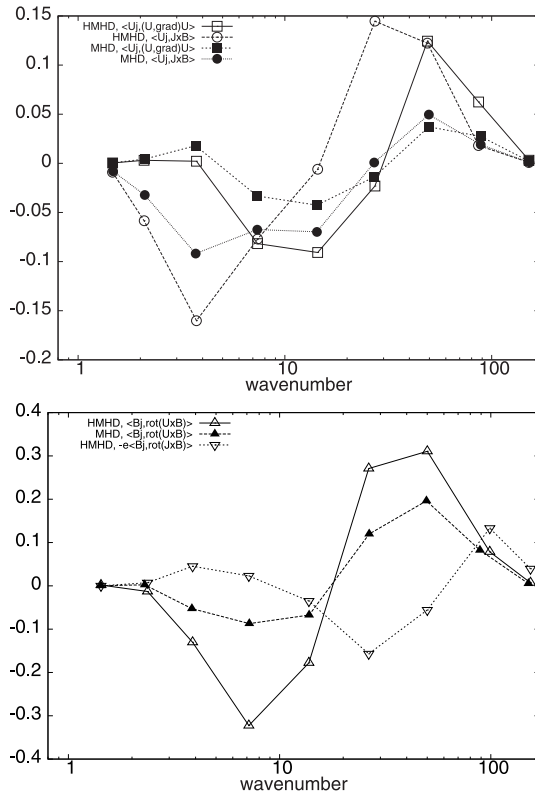


Fig. 2 Wavelet-scale spectra of energy transfer functions. Top: terms appearing in Eq. (5), bottom: those in Eq. (6). Squares:  $\langle u_j | u | u \rangle_{NL}$ , circles:  $\langle u_j | b | b \rangle_{Lor}$ , triangles:  $\langle b_j | b | u \rangle_{Ind}$ , and inverted triangles:  $\langle b_j | b | b \rangle_{Hall}$ . Abscissas of each quantity are the same as those in Fig. 1.

3. The peaks of the magnetic induction and Lorentz force effects on HMHD evolution are slightly shifted to smaller wavenumber modes compared with the MHD case.
4. The Hall term reduces the magnetic energy of moderate-scale components ( $j = 4, 5, 6$ ) and increases those of larger ones ( $0 \leq j \leq 3$ ) moderately and of smaller ones ( $j = 7, 8$ ) intensively.

## 5. Wavelet Scale-to-Scale Analysis of the Energy Budget between $E_j^{(u)}$ and $E_k^{(b)}$

In this section, we present more detailed features of the energy budget of the kinetic and magnetic energies. Figure 3 shows the spectra of the magnetic induction energy transfer brackets, which are given by  $\langle b_k | b | u_j \rangle_{Ind} := \sum_m \langle b_k | b_m | u_j \rangle_{Ind}$ . Although their average moduli differ, it is very remarkable that the following features are found in both the MHD and HMHD cases:

1. When  $j \geq k$ , i.e., the scales of the velocity components  $u_j$  are comparable to or smaller than those of the magnetic ones  $b_k$ , energy is transferred from  $b_k$  to  $u_j$ . On the other hand, when  $j < k$ , the direction is

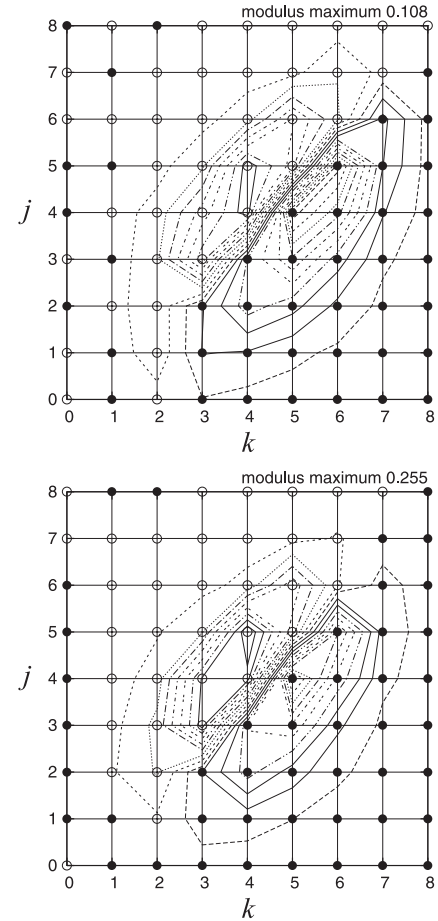


Fig. 3 Wavelet scale-to-scale energy transfer spectrum for magnetic induction:  $\langle b_k | b | u_j \rangle_{Ind}$ . Top: MHD case, bottom: HMHD case. Solid circles:  $\langle b_k | b | u_j \rangle_{Ind} > 0$ , i.e., the transfer enhances the magnetic energy  $E_k^{(B)}$ , open circles:  $\langle b_k | b | u_j \rangle_{Ind} < 0$ , i.e., the transfer enhances the kinetic energy  $E_j^{(u)}$ . Contours are added to clarify the transfer amplitudes. Levels of contours are given by  $(0.1n + 0.05) \times \max\{\langle b_k | b | u_j \rangle_{Ind}\}$ , where  $n$  is an integer.

reversed. Overall, energy is transferred from larger-scale components to smaller ones due to magnetic induction (or the Lorentz force) irrespective of the kind of field.

2. Intense transfer is localized around  $j \sim k$ . This implies that energy transfer is *local*; i.e., the transfer brackets that dominantly contribute to the energy budget are constituted by modes that have spatial scales very close to each other.

The dominance of local transfer is in sharp contrast to the results of Alexakis *et al.* [10], Mininni *et al.* [5], and our previous result [11], all of which report the importance of nonlocal energy transfer.

## 6. Influence of Hall Effect on the Energy Budget of $E_j^{(b)}$ Values

Figure 4 shows the wavelet scale-to-scale energy transfer spectrum for the Hall term effect  $\langle b_k | b | b_j \rangle_{Hall} :=$

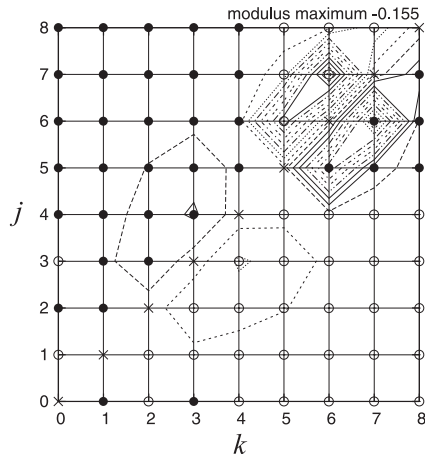


Fig. 4 Wavelet scale-to-scale energy transfer spectrum for the Hall term effect:  $\langle \mathbf{b}_k | \mathbf{b} | \mathbf{b}_j \rangle_{\text{Hall}}$ . Solid and open circles and contours have the same meaning as in Fig. 3. Crosses denote sites at which  $\langle \mathbf{b}_k | \mathbf{b} | \mathbf{b}_j \rangle_{\text{Hall}} \equiv 0$ .

$\sum_m \langle \mathbf{b}_k | \mathbf{b}_m | \mathbf{b}_j \rangle_{\text{Hall}}$ . Remarkably, the energy redistribution due to the Hall effect is also dominated by *local* transfers. It is also very interesting that the direction of energy transfer at smaller scales ( $j \geq 5$ ) is opposite to that at larger scales ( $j \leq 4$ ). At small scales, energy is intensively transferred to smaller scales; i.e., the Hall effect enhances the forward energy cascade. A moderate inverse energy cascade occurs at larger scales.

These results are qualitatively consistent with those found in Mininni *et al.*, which are based on Fourier analysis [5]. Quantitative comparison of our results with theirs does not seem straightforward because wavelet analysis has logarithmically mode-binding nature in wavenumber space, which is partly discussed in Ref. [6]. Their presentation, on the other hand, is based on linear binding in wavenumber space.

## 7. Detailed Analysis of the Magnetic Induction Bracket

In some sense, the brackets [Eqs. (8), (9), (12), and (13)] are wavelet counterparts of the so-called triad interaction in Fourier analysis of mode coupling. Figure 5 shows the distribution of the magnetic induction brackets  $\langle \mathbf{b}_k | \mathbf{b}_5 | \mathbf{u}_j \rangle_{\text{Ind}}$  as a typical example of the energy transfer tendency.

1. The scale of the to-mode  $\langle \mathbf{b}_k |$  of dominant interaction is very close to that of the by-mode  $|\mathbf{b}_m|$ , i.e.,  $k \sim m$ ,  $m \pm 1$ .
2. The intensive positive transfers are aligned on scales with  $k = m$  and  $m + 1$ . Negative ones are aligned on scales with  $k = m - 1$ .
3. The scale range of the from-mode  $|\mathbf{u}_j \rangle$  of significant interactions is rather broad, but the scales that give the maximum or minimum number of brackets are concentrated around  $m = 4$  or 5.

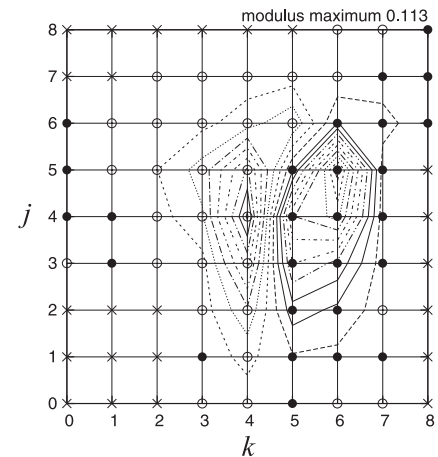
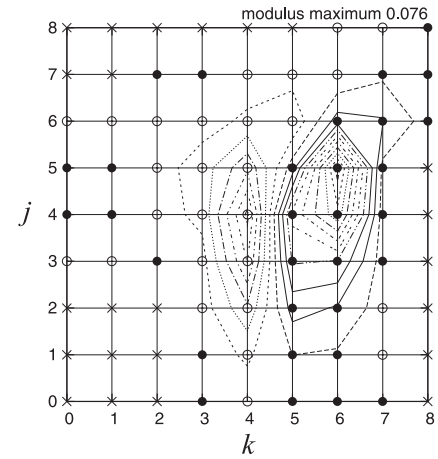


Fig. 5 Wavelet scale-to-scale energy transfer spectrum of the magnetic induction for an assigned by-mode  $|\mathbf{b}_5|$ :  $\langle \mathbf{b}_k | \mathbf{b}_5 | \mathbf{u}_j \rangle_{\text{Ind}}$ . Top: MHD case, bottom: HMHD case. Solid and open circles, cross symbols, and contours have the same meaning as in Figs. 3 and 4.

We confirmed that these features are seen in common for by-mode number  $m = 4, 5, 6, 7$ . It is remarkable and very interesting that although the peaks of the spectra for an assigned by-mode number  $m$  are aligned in the  $j$ -direction at some fixed  $k$  values, their superposition gives the distribution shown in Fig. 3, which is characterized by the concentrated alignment of peaks around  $j \sim k$ .

This work is performed under the auspices of the NIFS Collaboration Research program (NIFS07KTBL004).

- [1] K. Itoh *et al.*, Phys. Plasmas **12**, 062303 (2005).
- [2] S. M. Mahajan and Z. Yoshida, Phys. Plasmas **7**, 635 (2000).
- [3] S. Balbus and C. Terquem, Astrophys. J. **552**, 235 (2001).
- [4] J. Shiraishi, S. Ohsaki and Z. Yoshida, Phys. Plasmas **12**, 092901 (2005).
- [5] P. D. Mininni, A. Alexakis and A. Pouquet, J. Plasma Phys. **73**, 377 (2007).
- [6] K. Kishida, K. Araki, K. Suzuki and S. Kishiba, PRL **83**, 5487 (1999).
- [7] K. Araki and H. Miura, "Orthonormal Divergence-free Wavelet Analysis of Nonlinear Energy Transfer in Rolling-Up Vortices", Y. Kaneda (ed.), *IUTAM symposium on Com-*

- putational Physics and New Perspectives in Turbulence*, 149 (2008).
- [8] K. Araki and H. Miura, *J. Plasma Fusion Res. SERIES* **9**, 446 (2010).
- [9] H. Miura and D. Hori, *J. Plasma Fusion Res. SERIES* **8**, 73 (2009).
- [10] A. Alexakis, P. D. Mininni and A. Pouquet, *Phys. Rev. E* **72**, 046301 (2005).
- [11] K. Araki and H. Miura, *J. Plasma Fusion Res. SERIES* **8**, 96 (2009).